

The van der Waals rovibronic spectrum of *p*-difluorobenzene–Ar up to 125 cm⁻¹ intermolecular energy: Assignment and character of van der Waals modes

R. Sussmann and H. J. Neusser

*Institut für Physikalische und Theoretische Chemie, Technische Universität München, Lichtenbergstr. 4
85748 Garching, Germany*

(Received 20 October 1994; accepted 14 November 1994)

The van der Waals (vdW) vibronic spectrum built on the electronic $0_0^0, S_1(B_2) \leftarrow S_0(A_1)$ origin of *p*-difluorobenzene–Ar is investigated with rotational resolution ($\Delta\nu_{UV} = 60$ MHz). For the first time vdW vibronic bands are detected up to a van der Waals energy of 125 cm⁻¹ and assigned by a rotational analysis of the band structure. The band origin positions of the ten detected bands display a regular behavior with moderate anharmonicities and minor influences due to Fermi resonances. Using the concept of three-dimensional Kraitichman equations and of normalized effective planar moments characteristic data on the nuclear displacements in the two different bending coordinates are deduced from the measured rotational constants. The fundamental vdW vibronic states at low energies can be described in terms of one-dimensional normal modes while vdW states at higher energies display mixed mode character. © 1995 American Institute of Physics.

I. INTRODUCTION

Two central goals of the spectroscopy of van der Waals (vdW) complexes concern their *structure* and the exploration of their *intermolecular motions*. Accurate information on the structure of the prototype complexes of an aromatic molecule and noble gas atoms has emerged from rotationally resolved investigations in the UV spectral region. First examples were *s*-tetrazine complexed with one and two Ar atoms (Refs. 1 and 2) and benzene–(Ar)_{*n*} (*n* = 1, 2) (Refs. 3–5) which proved a central binding position of the Ar atom at a distance of 3.58 Å in the *S*₀ state of benzene–Ar. Measurements have been extended to larger aromatic (two and more rings) substrates complexed by two and more Ar atoms only recently.^{6–9} These investigations clearly show that an opposite-sided binding topology with central noble gas atoms is favored and no dropletlike Ar subclusters are likely to be formed on one side of the aromatic substrate.

In contrast to the advanced knowledge of the structures our understanding of the intermolecular motions within the aromatic–noble gas complexes is far from complete. The van der Waals mode structure of the *S*₁ ← *S*₀ transition in aromatic molecule–atom complexes has been studied by vibrationally resolved vibronic spectroscopy providing no rotational resolution. van der Waals vibronic spectra of benzene–Ar (Ref. 10), monosubstituted benzene–Ar complexes (Refs. 11 and 12), *s*-tetrazine–Ar (Refs. 13 and 14), carbazole–Ar (Ref. 15), fluorene–Ar (Ref. 16), and naphthalene–Ar (Ref. 17) have been reported.

First quantum mechanical three-dimensional (3D) calculations of bound vdW rovibrational states in clusters involving *aromatic molecules* have been performed for benzene–Ar and *s*-tetrazine–Ar as early as in 1986.¹⁸ However, it turned out that the expansion of the (empirical) intermolecular potential in spherical harmonics works better for the nonaromatic complex NH₃–Ar.¹⁹ Very recently the multidimensional intermolecular potential energy surface of NH₃–Ar has been determined from experimental data.²⁰ For *aromatic*

molecule–noble gas complexes Brocks and van Koeven derived a vdW vibrational Hamiltonian in the body fixed frame.²¹ This approach has been applied using different basis sets for fluorene–Ar (Ref. 21) and benzene–Ar (Refs. 22 and 23). Either empirical potentials or analytic representations of *ab initio* potential surfaces were used in these 3D quantum mechanical calculations. By this means in very recent work vibrationally resolved vdW vibronic spectra of aniline–Ar (Ref. 24), (4 fluoro-)styrene–Ar (Ref. 25), and (2,3 dimethyl-)naphthalene–Ar (Refs. 26 and 27) were interpreted.

For a critical test of theoretical results on the vibrational wave function rotationally resolved experimental spectra of vdW vibronic states are required. Rotational constants obtained in this way are the result of an averaging of the vibrational motion and thus contain information on the average displacements during the intermolecular vibration. Hitherto, only two examples for vdW vibronic spectra with rotational resolution have been reported. In *s*-tetrazine–Ar, Levy and co-workers obtained rotational contours of the origin band and one vdW vibronic band involving the stretching vibration,²⁸ theoretical work was performed by Tiller and Clary.²⁹ Champagne *et al.* obtained highly resolved UV spectra of vdW bands in *trans*-stilbene–Ar.³⁰ For benzene–Ar rotational resolution has been achieved for all three vdW vibronic bands known from low resolution spectroscopy.^{5,31} The complete rotational analysis of these vibronic bands will be presented elsewhere^{5,31} and compared with the calculations of the rovibrational states.^{22,23}

In this work the high resolution spectra of several van der Waals vibronic bands of another model system, *p*-difluorobenzene–Ar (*p*DFB–Ar) are presented leading to a complete analysis of the vdW vibrations. This complex is of particular interest because its reduced symmetry leads to spectra without degenerate modes and the electronic origin becomes electronically allowed. In recent work we found a vdW bond length of 3.55 Å in *p*DFB–Ar in the *S*₀ state,³²

and presented rotationally resolved spectra of the two lowest energy vdW vibronic bands.³³ We found proof for a Herzberg–Teller activity of the short in-plane vdW bending mode b_y at $+34\text{ cm}^{-1}$. In this work the assignment of eight additional vdW vibronic bands up to a vdW excess energy of 0_0^0+125 cm^{-1} will be derived from the analysis of their rotational band structure. From the fitted rotational constants information on the typical displacements is derived.

II. EXPERIMENT

The experimental setup for recording rotationally resolved spectra of *p*DFB–Ar complexes with the technique of mass-selective resonance-enhanced two-photon ionization has been described in detail in our previous work.³² Briefly, for the first narrow-band excitation step the light of a cw single mode laser (Coherent 699/21) is pulsed amplified in excimer laser-pumped dye cells yielding nearly Fourier transform-limited 1 mJ light pulses with a duration of 20 ns [full width at half maximum (FWHM)] and a frequency width of 60 MHz (FWHM) after frequency doubling. For ionization a broadband excimer-pumped dye laser (Lambda Physik FL 2002) is used with a pulse energy of 1 mJ. The laser light beams were attenuated by a factor of 10–50 to avoid saturation and line broadening. The wavelength of the (second) ionization laser had to be chosen carefully, since the second excitation step to the ionization continuum requires a higher photon energy than the first step and could lead to a one-color signal. *p*-Difluorobenzene at a concentration of 1% is seeded in Ar at a backing pressure of 2 bar and the mixture is expanded through a solenoid valve with a 300 μm orifice into the vacuum chamber. A skimmer of 1.5 mm diameter placed 4 cm downstream reduces the residual Doppler width below the laser linewidth, and the ionized complexes are mass separated in a homemade time of flight mass spectrometer.

III. THE MODEL SYSTEM *p*DFB–Ar

In the prototype aromatic molecule–noble gas complex, benzene–Ar, only three vdW vibronic bands on the blue side of the 6_0^1 transition were found at vdW excess energies of $+31$, $+40$, and $+63\text{ cm}^{-1}$ in spectra with vibrational resolution¹⁰ and rotational resolution.^{5,31} Thus, the region of overlap suitable to compare with theoretical vdW rovibrational states calculated from the *ab initio* potential (well

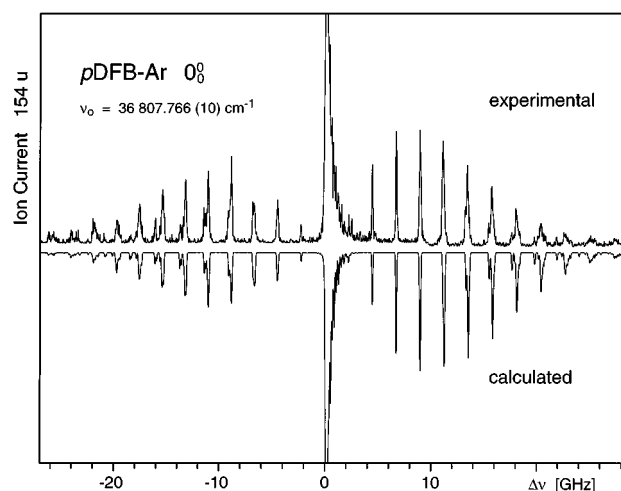


FIG. 1. Upper trace: Rotationally resolved spectrum of the 0_0^0 ($S_1 \leftarrow S_0$) transition of the *p*-difluorobenzene–Ar vdW complex obtained by recording the ion current at mass 154 u as a function of the frequency of the laser providing the first photon in the two-photon ionization process. Lower inverted trace: Theoretical *c*-type rotational spectrum of a near oblate asymmetric top calculated with the rotational constants resulting from the best fit to the experimental spectrum (Table I) (taken from Ref. 33).

depth 429 cm^{-1}) (Ref. 34) is small. Higher vdW vibronic states are needed for this comparison. In this work we will demonstrate that *p*DFB–Ar is suitable for detection of high lying vdW vibronic bands due to its lower symmetry and the parallel-type rotational structure of most of the bands. The rotational structure of the parallel-type bands with a strong *Q*-branch peak is different from the perpendicular band structure of vdW vibronic bands in benzene–Ar. It will be shown that this leads to an increased sensitivity for the detection of additional quanta of weak vdW transitions.

The one-photon electronic transition $S_1(^1B_2) \leftarrow S_0(^1A_1)$ in *p*DFB–Ar (C_{2v}) is electric dipole allowed with a transition moment directed along the short in-plane $y(\parallel c)$ axis; i.e., a *c*-type rotational band is observed. The spectrum of the 0_0^0 band in *p*DFB–Ar is shown in the upper trace of Fig. 1.³³ Its rotational structure with a strong blue-shaded *Q* branch and well separated *P*- and *R*-branch subgroups in the wings of the band is characteristic of a parallel-type band. The rotational analysis of this spectrum was described in detail in our recent work,³² and the resulting rotational constants are

TABLE I. Wave numbers of the band origins ν_0 , vibrational shifts $\delta\nu$, asymmetry parameters κ , and rotational constants of *p*-difluorobenzene–Ar in its ground electronic (0_0), electronically (0^0), and vibrationally (30^1) excited states. Indicated errors of the rotational constants reflect the uncertainty of the $\Delta A = A' - A''$, ΔB , and ΔC values resulting from the fit procedure.

0_0 state ^a		0^0 state ^a		30^1 state	
	ν_0 (cm^{-1})	36 807.766(10)	ν_0 (cm^{-1})	36 927.646(10)	
			$\delta\nu$ (cm^{-1})	+119.880(15)	
A_0'' (cm^{-1})	0.038 01	A_0' (cm^{-1})	0.037 65(10)	A_v' (cm^{-1})	0.037 89(10)
B_0'' (cm^{-1})	0.036 45	B_0' (cm^{-1})	0.036 90(10)	B_v' (cm^{-1})	0.036 30(10)
C_0'' (cm^{-1})	0.023 20	C_0' (cm^{-1})	0.023 55(3)	C_v' (cm^{-1})	0.023 45(5)
κ_0'	+0.789	κ_0'	+0.894		

^aTaken from Ref. 32.

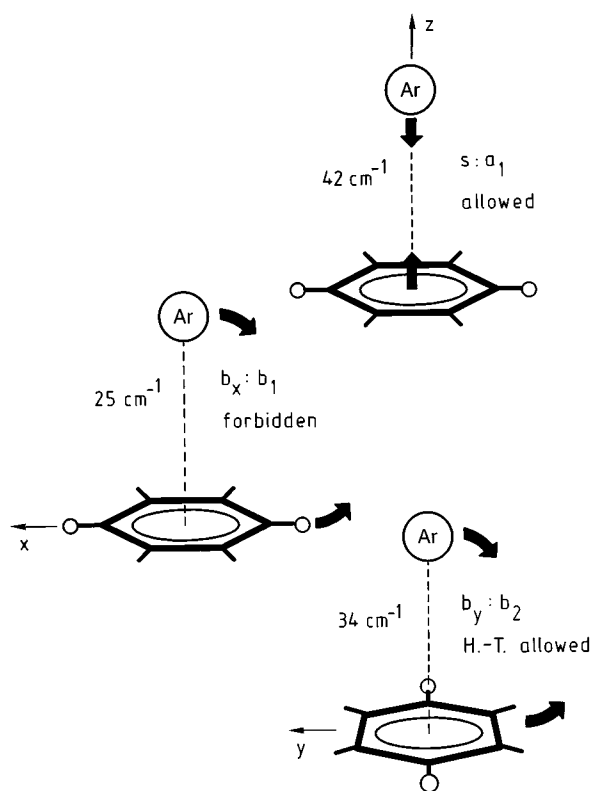


FIG. 2. Structure of the *p*-difluorobenzene–Ar vdW complex of point group C_{2v} with the axes $x(\parallel b)$, $y(\parallel c)$, $z(\parallel a)$. The Ar atom is located on the C_2 axis at an effective vdW distance of 3.55 Å from the molecular plane. The arrows indicate the relative motions of the *p*DFB molecule and the Ar atom when the vdW stretching mode s (a_1), the long in-plane bending mode b_x (b_1), and the short in-plane bend b_y (b_2) are excited. The indicated wave numbers are the vibrational shifts of the vdW vibronic spectra discussed in this work. The possibility of single quantum excitation in the S_1 state is indicated, including Herzberg–Teller coupling by vdW modes (for an explanation, see the text).

presented in Table I. A theoretical stick spectrum convoluted with a 120 MHz (FWHM) Gaussian function was calculated from these rotational constants and for a rotational temperature of 1.5 K. It is shown in the lower inverted trace of Fig. 1 and represents the vibronic c -type spectrum of a near oblate ($\kappa'' = +0.789$) asymmetric rotor with the electronic transition dipole moment polarized along the short in-plane axis of the *p*DFB molecule (see Fig. 2). The c -type rotational selection rules are $(ee) \leftrightarrow (oe)$ and $(eo) \leftrightarrow (oo)$ for (K_{-1}, K_{+1}) , where e, o denotes the even and odd parity, respectively. The nuclear spin statistical weights for the structure discussed below are $g_n = 14$ for $(K''_{-1}, K''_{+1}) = (ee), (eo)$ and $g_n = 18$ for $(K''_{-1}, K''_{+1}) = (oe), (oo)$. For the wave number of the rotationless origin of the band we found $\nu_0 = 36\,807.766(10) \text{ cm}^{-1}$.

The structure of *p*DFB–Ar derived from the rotational spectrum is presented in Fig. 2. In the electronic ground state S_0 the Ar atom is found to be placed on the C_2 axis of the bare molecule at an effective van der Waals distance of $z''_{\text{eff}} = 3.55(2) \text{ Å}$.³² This is reduced by 0.06 Å after electronic excitation to the S_1 state. The decrease of the vdW bond length can be visualized from the blue shading of the Q

TABLE II. Frequency shifts, intensities (very strong, vs; strong, s ; weak, w ; very weak, vw) of bands in the rovibronic spectrum of *p*DFB–Ar and their assignment.

Frequency shift (cm^{-1})	Relative intensity	Assignment
0.0 ^a	vs	0_0^0
1.860(20)	w	
4.140(20) ^b	w	22_1^1
33.695(15) ^a	s	b_{y0}^1
41.549(10) ^a	s	s_0^1
43.425(20)	vw	
45.679(20)	vw	$s_0^1 22_1^1$
50.593(15)	w	b_{x0}^2
65.876(15) ^a	s	b_{y0}^2
80.652(10)	w	s_0^2
89.617(15)	vw	$s_0^1 b_{x0}^2$
95.95(10)	vw	b_{y0}^3
99.105(15)	vw	b_{x0}^4
117.133(15)	vw	s_0^3
119.880(15) ^a	vs	30_0^1
124.348(20)	vw	$30_0^1 22_1^1$
125.562(15)	vw	b_{y0}^4

^aPreviously these transitions have been also detected in low resolution (Ref. 35).

^bPreviously this transition has been also detected in low resolution in the bare *p*DFB molecule (Ref. 42).

branch, and the peaks in the R branch which are narrower and higher than in the P branch.

IV. THE vdW ROVIBRONIC SPECTRUM OF *p*DFB–Ar

Three vdW vibronic bands located at +34, +42, and +66 cm^{-1} to the blue of the electronically allowed origin are known from vibrationally resolved spectroscopy.³⁵ In the high resolution scan because of the sharp central Q branch and the regular P - and R -branch substructure we found a large number of vibronic bands within 125 cm^{-1} to the blue of the 0_0^0 band, which are weaker by a factor of 10–100 than the 0_0^0 band and thus were not detected in earlier low resolution investigations.^{35,36} The observed frequency positions are listed in Table II. We found 16 bands in this frequency range. Ten of these are assigned as vdW vibronic transitions. The most prominent of the remaining bands is the 30_0^1 band with a c -type rotational structure at +119.880(15) cm^{-1} (Table I). ν_{30} is a skeletal b_{2g} (D_{2h}) vibration whose symmetry species is reduced to a_1 in the complex (C_{2v}). The c -type rotational structure observed in this work corroborates the assignment of this band in previous work.³⁷

In Fig. 2 the relative motions of the *p*DFB molecule and the Ar atom are shown for the three possible intermolecular modes. These are the totally symmetric stretching mode s (a_1) leading to a displacement perpendicular to the aromatic ring and two bending modes ($b_{x,y}$) with a displacement perpendicular to the vertical rotational axis. While the bending modes $b_{x,y}$ (e_1) are degenerate in benzene–Ar, the degeneracy is lifted in *p*DFB–Ar (C_{2v}) leading to a *long* in-plane bend (b_1) and a *short* in-plane bending mode (b_2), which are different in frequency.

Vibronic transitions leading to a_1 fundamental vibrational states, to combinations and overtones of a_1 vibrations,

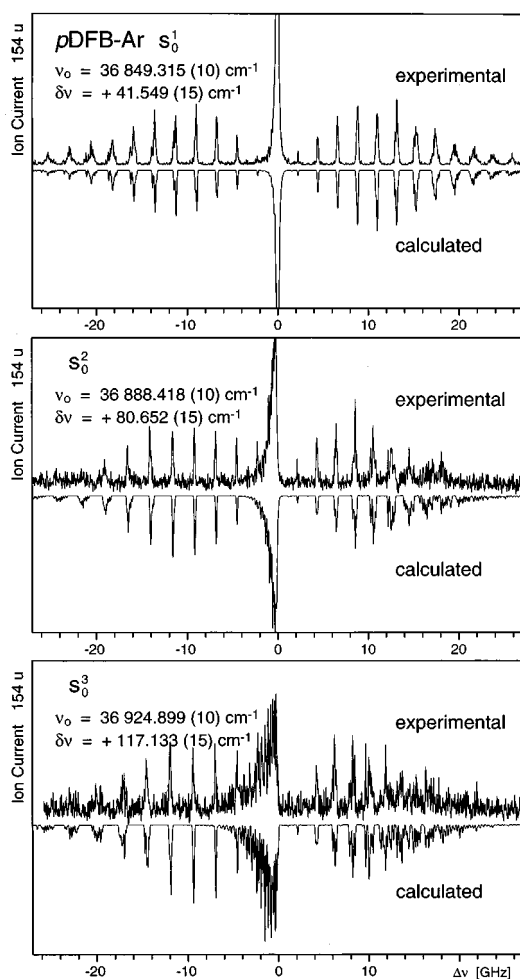


FIG. 3. Rotationally resolved spectra of the s_0^1 (upper), s_0^2 (middle), and s_0^3 (lower) ($S_1 \leftarrow S_0$) transitions leading to excited states of the vdW stretching mode of the *p*-difluorobenzene–Ar vdW complex. Simulations of the experimental spectra by calculated *c*-type rotational spectra of a near oblate asymmetric top are shown in the inverted traces.

or to odd overtones of nontotally symmetric vibrational species are symmetry allowed, can be Franck–Condon active, and display a *c*-type rotational structure.

A. van der Waals stretching modes

1. s_0^1 , s_0^2 , s_0^3 bands

We assign the *c*-type bands with origins at +41.549(15), +80.652(15), and +117.133(15) cm^{-1} to the s_0^1 , s_0^2 , and s_0^3 transitions, respectively. Their rotational structure is shown in Fig. 3. The rotational constants of the final states change in a way that leads to an increasing red-shading of the sharp central Q branch with increasing stretching quantum number. The fitted best set of rotational constants is used for the theoretical spectra displayed on the inverted lower trace.

The assignment of the s_0^1 band agrees with the result of previous work.^{35,36} It is in line with the assignment of s_0^1 bands of benzene–Ar (Refs. 5 and 10) and *s*-tetrazine–Ar (Refs. 13, 14, and 28). Neglecting influences from possible Fermi resonances (see Sec. V), a one-dimensional cubic ex-

TABLE III. Band origins ν_0 , vibrational shifts $\delta\nu$, and rotational constants A'_{vdW} , B'_{vdW} , C'_{vdW} of stretching vdW vibronic states. δA : = $A'_{\text{vdW}} - A_0$, $\delta B'$, and $\delta C'$ are the deviations of the rotational constants of the vdW vibronic state from the respective values of the 0^0 state. Changes of planar moments $\delta P_{x,y}^{\text{eff}}$, effective vdW bond length z_{eff} , and change δz_{eff} of the vdW vibronic states.

	s^1 state	s^2 state	s^3 state
ν_0 (cm^{-1})	36 849.315(10)	36 888.418(10)	36 924.899(10)
$\delta\nu$ (cm^{-1})	+41.549(15)	+80.652(15)	+117.133(15)
Trans. dipole	<i>c</i> -type	<i>c</i> -type	<i>c</i> -type
A'_{vdW} (cm^{-1})	0.037 70(10)	0.037 65(15)	0.037 40(15)
δA (cm^{-1})	+0.000 05(15)	\pm 0.000 00(18)	−0.000 25(18)
B'_{vdW} (cm^{-1})	0.036 15(10)	0.035 30(15)	0.034 40(15)
δB (cm^{-1})	−0.000 75(15)	−0.001 60(18)	−0.002 50(18)
C'_{vdW} (cm^{-1})	0.023 30(3)	0.022 92(5)	0.022 37(5)
δC (cm^{-1})	−0.000 25(5)	−0.000 62(6)	−0.001 18(6)
δP_x^{eff} ($\text{u}\text{\AA}^2$)	−1.196	−0.516	+3.775
δP_y^{eff} ($\text{u}\text{\AA}^2$)	+0.602	+0.516	−0.783
z_{eff} (\AA)	3.53	3.59	3.65
δz_{eff} (\AA)	+0.04	+0.10	+0.16

trapolation of the frequency shifts of the s^1 , s^2 , and s^3 states (Table III) yields $D_e(\text{stretch}) \approx 300 \text{ cm}^{-1}$, with the harmonic frequency $\omega_e = 42.2 \text{ cm}^{-1}$, the (diagonal) anharmonicities $\omega_e x_e = +1.091 \text{ cm}^{-1}$, and $\omega_e y_e = -0.029 \text{ cm}^{-1}$. We deduce further evidence for the validity of this assignment from the rotational constants of these bands.

2. s^n rotational constants

Generally, there are three major contributions to the rotational constants which reflect three different kinds of vibration–rotation interaction:³⁸ (i) harmonic contribution due to “inverse vibrational averaging,” (ii) anharmonicity, or more general, asymmetry of a potential, and (iii) Coriolis coupling.

The experimentally determined rotational constants A'_{vdW} , B'_{vdW} , C'_{vdW} (Table III) are plotted as a function of the vdW vibrational stretching quantum number ν_s in Fig. 4(a).

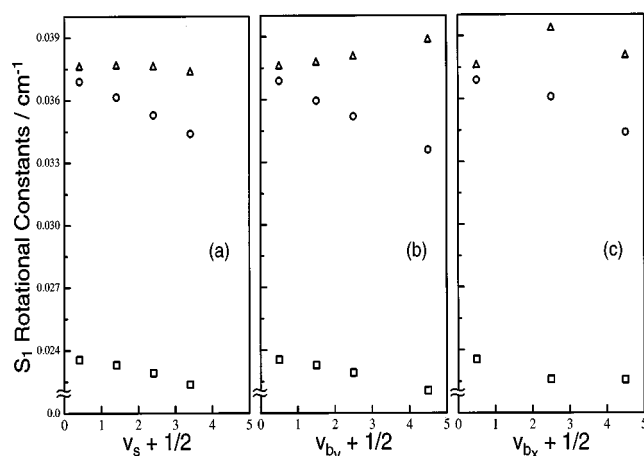


FIG. 4. Evolution of measured S_1 rotational constants, A'_{vdW} (Δ), B'_{vdW} (\circ), C'_{vdW} (\square) for an increasing number of excited quanta of the vdW stretching modes (a), short in-plane bending modes (b), and long in-plane bending modes (c). For an explanation, see the text.

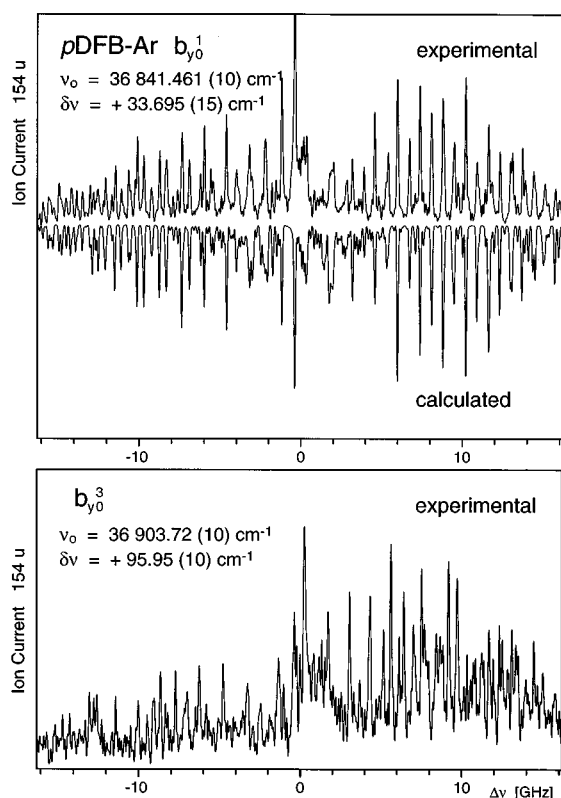


FIG. 5. Rotationally resolved spectra of the $b_{y_0}^1$ (upper) and $b_{y_0}^3$ (lower) ($S_1 \leftarrow S_0$) transitions involving odd quanta of the Herzberg–Teller active short in-plane vdW bending mode of the *p*-difluorobenzene–Ar vdW complex. A simulation of the experimental spectrum by a calculated *a*-type rotational spectrum of a near oblate asymmetric top is shown in an inverted trace for the $b_{y_0}^1$ transition (upper).

Note that we find $A'_{\text{vdW}} \approx B'_{\text{vdW}}$ for $v_s=0$ indicating that *p*DFB–Ar is a near oblate ($\kappa'_0 = +0.894$) asymmetric top. This equality is increasingly perturbed by excitation of vdW vibrations. The B'_{vdW} and C'_{vdW} rotational constants decrease with increasing v_s due to effective moments of inertia I_b^{eff} and I_c^{eff} increasing by harmonic and anharmonic vibration–rotation interaction. On the contrary, the A'_{vdW} constant remains nearly unchanged (see the small values for $\delta A: = A'_{\text{vdW}} - A'_0$ in Table III). This is reasonable since the *a* axis is collinear to the vdW stretching coordinate and I_a^{eff} is not influenced by intermolecular displacements along this coordinate. The constant A'_{vdW} value (up to $v_s=3$) demonstrates that no displacements perpendicular to the *z* coordinate are involved in the excited states and stretch–bend coupling is small. It also corroborates our assignment as s_0^1 , s_0^2 , s_0^3 transitions.

B. Short in-plane bending vibrations: Herzberg–Teller active vdW modes

The bands with origin at +33.695(15) and +95.95(10) cm^{-1} shown in Fig. 5 display a rotational structure completely different from the *c*-type found for all other bands in Figs. 1, 3, 6, and 7.

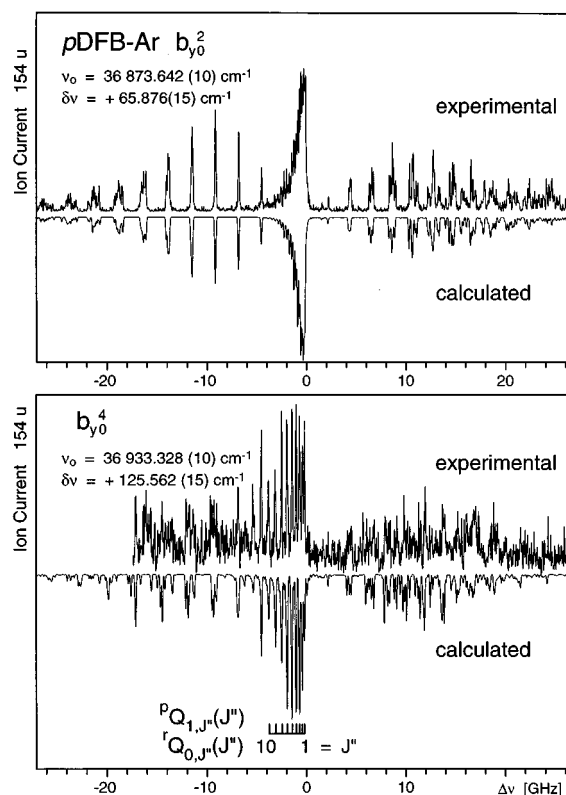


FIG. 6. Rotationally resolved spectra of the $b_{y_0}^2$ (upper) and $b_{y_0}^4$ (lower) ($S_1 \leftarrow S_0$) transitions involving even quanta of the short in-plane vdW bending mode of the *p*-difluorobenzene–Ar vdW complex. Simulations of the experimental spectra by calculated *c*-type rotational spectra of a near oblate asymmetric top are shown in the inverted traces. For the $b_{y_0}^4$ band the *Q* subbranches are indicated.

1. $b_{y_0}^1$ band

Recently, we have shown that the band at +33.695(15) cm^{-1} can be simulated with *a*-type rotational selection rules (see Fig. 5).³³ This excludes the assignment as a first bending overtone b_0^2 (which should display a *c*-type band structure). Furthermore, from the regular well reproduced rotational structure we can exclude Coriolis coupling to the s^1 state as the origin for the appearance of this band. The unperturbed *a*-type rotational structure is proof for the Herzberg–Teller (HT) induced activity of this band.³³

2. $b_{y_0}^3$ band

The structure of the band at +95.95(10) cm^{-1} (lower trace of Fig. 5) is much closer to the *a*-type structure than to a *c*-type structure (see, e.g., the strong peak in the center and the periodic structure on the blue side). For this reason we assign it to the $b_{y_0}^3$ band.

3. $b_{y_0}^2$, $b_{y_0}^4$ bands

The bands with origin at +65.876(15) and +125.562(15) cm^{-1} display a clear *c*-type structure (see Fig. 6). We assign them to the $b_{y_0}^2$ and the $b_{y_0}^4$ transition, respectively. The $b_{y_0}^4$ band with an excess energy of +125.562(15)

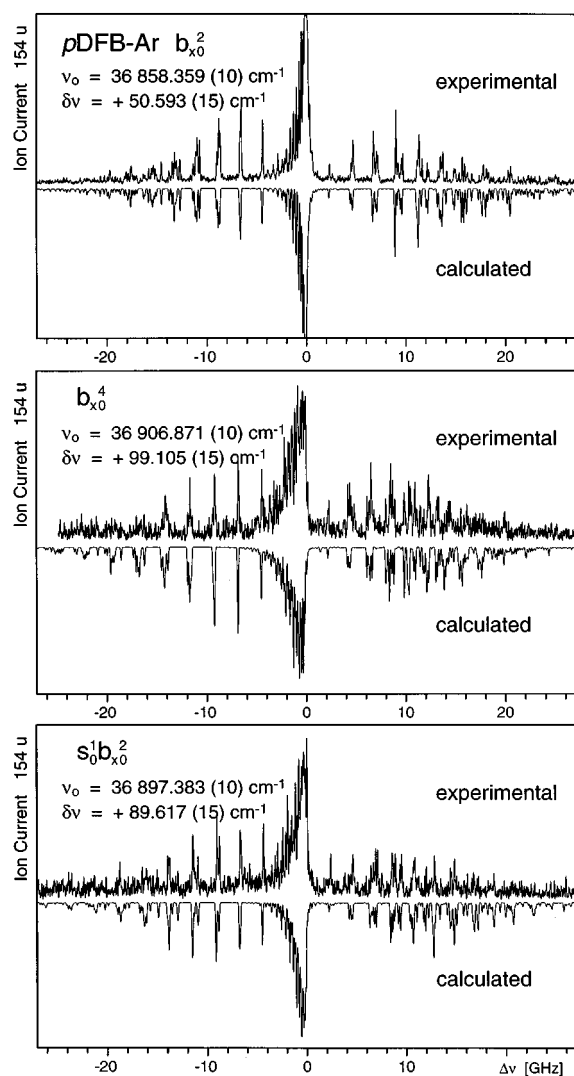


FIG. 7. Rotationally resolved spectra of the b_{x0}^2 (upper) and b_{x0}^4 (middle) ($S_1 \leftarrow S_0$) transitions involving even quanta of the long in-plane vdW bending mode, and the $s_0^1 b_{x0}^2$ transition (lower) involving the fundamental stretch and long in-plane bending overtone combination mode of the *p*-difluorobenzene–Ar vdW complex. Simulation of the experimental spectra by calculated *c*-type rotational spectra of a near oblate asymmetric top are shown in the inverted traces.

cm^{-1} is the highest energy vdW vibronic band found in our experiment. Vibration–rotation interaction leads to a strongly red shaded Q branch so that single J'' values are resolved [the asymmetry splitting between the ${}^P Q_{1,J''}(J'')$ and ${}^R Q_{0,J''}(J'')$ subbranches is less than the experimental linewidth]. Congestion in the P branch of the experimental b_{y0}^4 spectrum is caused by the overlapping R branch of the 30_0^1 band whose origin is only $5.68(2) \text{ cm}^{-1}$ located to the red (Table I).

4. b_y^n rotational constants

The A'_{vdW} constants of the b_y^n vibronic states (Table IV) display a monotonous increase as a function of vibrational quantum number ν_{b_y} [see Fig. 4(b)]. This is different from the behavior of the A'_{vdW} constant of the stretching mode and

clearly demonstrates that a librational motion³⁹ is involved, with a (hindered) rotational motion of the substrate within the complex, thus corroborating the bending assignment of the vibration. The increase of A'_{vdW} is *not* caused by anharmonicity, since this could only lead to *decreasing* rotational constants. Thus, harmonic vibrational averaging of the bending wave function is the origin of increasing A'_{vdW} constants. On the other hand, the monotonous *decrease* of the B'_{vdW} and C'_{vdW} constants is due to harmonic and/or anharmonic contributions.

C. Long in-plane bending vibrations

1. b_{x0}^2 and b_{x0}^4 bands

The bands with origin at $+50.593(15)$ and $+99.105(15) \text{ cm}^{-1}$ (see Fig. 7) are assigned to the b_{x0}^2 and b_{x0}^4 transitions. The forbidden b_x mode (b_1) *cannot* be HT active by symmetry. It can be only excited as even quanta in the $S_1 \leftarrow S_0$ transition; i.e., the fundamental b_{x0}^1 is missing in our spectrum. Considering the bending modes as *librational* modes, with a large part of mode energy due to (hindered) rotational motion of the substrate within the complex, a significant reduction of the (benzene–Ar) bending frequency is expected, if hydrogen atoms are *p*-disubstituted by fluorine in *p*DFB–Ar. For the bending mode, b_x , a displacement of the heavy halogen atoms is involved. Thus a lower b_x frequency than in benzene–Ar is expected in agreement with the experimental b_x frequency of about 25 cm^{-1} significantly below the value of about 34 cm^{-1} found for the b_y fundamental.

2. $s_0^1 b_{x0}^2$ band

At this point there is only one remaining vdW vibronic band to be assigned. This is the *c*-type band with origin at $+89.617(15) \text{ cm}^{-1}$ (see Fig. 7). Its position agrees quite well with the sum of the frequencies of the b_x^2 and the s_0^1 state and is thus assigned to the $s_0^1 b_{x0}^2$ combination band.

3. b_x^n rotational constants

As expected for bending vibrations the dependence of rotational constants A'_{vdW} , B'_{vdW} , C'_{vdW} (Table V) on excited b_x quanta [see Fig. 4(c)] shows a similar behavior as found for the b_y^n states between $n=0$ and $n=4$ [see Fig. 4(b)]. However, disagreement is found for the A'_{vdW} and C'_{vdW} constants of the b_x^4 state [see Fig. 4(c)] showing a nonmonotonous behavior. This can no longer be attributed solely to harmonic and/or anharmonic effects but rather to a selective Coriolis coupling. Considering Jahn's rule,⁴⁰ $\Gamma(b_x^4) \otimes \Gamma(b_y^3) = \Gamma(R_x^4)$, we find that second order Coriolis coupling to the very weak HT active b_y^3 state only $3.16(10) \text{ cm}^{-1}$ to the red is possible.

D. Mode character

The frequency shifts of all discussed vdW vibronic bands are displayed in Fig. 8 as a function of their vdW vibrational quantum number. The goal of this section is to elucidate the character of these vibrational motions. In particular, the mixing of bending and stretching modes for higher quanta will be discussed.

TABLE IV. Band origins ν_0 , vibrational shifts $\delta\nu$, and rotational constants A'_{vdW} , B'_{vdW} , C'_{vdW} of short in-plane bending vdW vibronic states. δA : = $A'_{\text{vdW}} - A'_0$, $\delta B'$, and $\delta C'$ are the deviations of the rotational constants of the vdW vibronic state from the respective values of the 0^0 state. Changes of planar moments $\delta P_{x,y}^{\text{eff}}$, effective vdW bond length z'_{eff} , and change δz_{eff} of the vdW vibronic states.

	b_y^1 state	b_y^2 state	b_y^3 state	b_y^4 state
ν_0 (cm $^{-1}$)	36 841.461(10)	36 873.642(10)	36 903.72(10)	36 933.328(10)
$\delta\nu$ (cm $^{-1}$)	+33.695(15)	+65.876(15)	+95.95(10)	+125.562(15)
Trans. dipole	<i>a</i> -type	<i>c</i> -type	<i>a</i> -type	<i>c</i> -type
A'_{vdW} (cm $^{-1}$)	0.037 82(10)	0.038 10(10)		0.038 90(10)
δA (cm $^{-1}$)	+0.000 17(15)	+0.000 45(15)		+0.001 25(15)
B'_{vdW} (cm $^{-1}$)	0.035 95(10)	0.035 20(10)		0.033 60(10)
δB (cm $^{-1}$)	-0.000 95(15)	-0.001 70(15)		-0.003 30(15)
C'_{vdW} (cm $^{-1}$)	0.023 28(5)	0.022 92(3)		0.022 07(3)
δC (cm $^{-1}$)	-0.000 27(7)	-0.000 63(5)		-0.001 48(5)
δP_x^{eff} ($u\text{\AA}^2$)	-2.891	-3.838		-5.627
δP_y^{eff} ($u\text{\AA}^2$)	+0.879	-1.450		-8.761
z'_{eff} (\AA)	3.54	3.55		3.53
δz_{eff} (\AA)	+0.05	+0.06		+0.04

Vibration–rotation interaction results in an increase, $\delta z_{\text{eff}} = z'_{\text{eff}}(\text{vdW vibronic state}) - z'_{\text{eff}}(0^0)$, of the effective vdW bond length (along the stretching coordinate) with increasing intermolecular energy for the vdW vibronic states s^1 , s^2 , and s^3 (Table III). While excitation of the short in-plane bending modes (Fig. 2) does not affect the intermolecular distance (Table IV), the excitation of the long in-plane bending overtone (Fig. 2) results in a large value of δz_{eff} (Table V). This indicates bend–stretch coupling. The consideration of effective coordinates x'_{eff} and y'_{eff} , using three-dimensional Kraitchman equations,³⁸ is not instructive since their calculation partially leads to imaginary values for the higher vibrational states, as found for similar cases. Thus we apply an analysis of planar moments $P_{x,y,z}^e$. Planar moments of a rigid nonplanar molecule with moments of inertia $I_{x,y,z}^e$ are defined as

$$P_x^e = \frac{1}{2}(I_y^e + I_z^e - I_x^e) = \sum_i m_i x_i^2, \quad (1)$$

where x_i is one Cartesian coordinate of the i th atom. Expressions for P_y^e and P_z^e are obtained by cyclic permutation of the subscripts x , y , z . Employing effective moments of inertia, $I_{x,y,z}^{\text{eff}}$, the resulting effective planar moments contain contributions from vibration–rotation interactions and Eq. (1) is replaced by

$$2P_x^{\text{eff}} = I_y^{\text{eff}} + I_z^{\text{eff}} - I_x^{\text{eff}} = 2P_x^e - \Delta_x, \quad (2)$$

where Δ_x represents the pseudoinertial defect, containing generally harmonic and anharmonic vibrational contributions.⁴¹ Large values of $\Delta_{x,y,z}$ indicate major effects due to vibration–rotation coupling, i.e., in the absence of Coriolis coupling this means strong harmonic and/or anharmonic vibrational averaging.

TABLE V. Band origins ν_0 , vibrational shifts $\delta\nu$, and rotational constants A'_{vdW} , B'_{vdW} , C'_{vdW} of vdW vibronic states involving the long in-plane bend. δA : = $A'_{\text{vdW}} - A'_0$, $\delta B'$, and $\delta C'$ are the deviations of the rotational constants of the vdW vibronic state from the respective values of the 0^0 state. Changes of planar moments $\delta P_{x,y}^{\text{eff}}$, effective vdW bond length z'_{eff} , and change δz_{eff} of the vdW vibronic states.

	b_x^2 state	b_x^4 state ^a	$s^1 b_x^2$ state
ν_0 (cm $^{-1}$)	36 858.359(10)	36 906.871(10)	36 897.383(10)
$\delta\nu$ (cm $^{-1}$)	+50.593(15)	+99.105(15)	+89.617(15)
Trans. dipole	<i>c</i> -type	<i>c</i> -type	<i>c</i> -type
A'_{vdW} (cm $^{-1}$)	0.039 40(10)	0.038 10	0.039 30(10)
δA (cm $^{-1}$)	+0.001 75(15)	+0.000 45	+0.001 65(15)
B'_{vdW} (cm $^{-1}$)	0.036 10(10)	0.034 40	0.034 90(10)
δB (cm $^{-1}$)	-0.000 80(15)	-0.002 50	-0.002 00(15)
C'_{vdW} (cm $^{-1}$)	0.022 60(3)	0.022 57	0.022 52(3)
δC (cm $^{-1}$)	-0.000 95(5)	-0.000 98	-0.001 03(5)
δP_x^{eff} ($u\text{\AA}^2$)	-0.039	-3.704	-6.120
δP_y^{eff} ($u\text{\AA}^2$)	-19.926	-1.584	-12.679
z'_{eff} (\AA)	3.22	3.60	3.38
δz_{eff}	-0.27	+0.11	-0.11

^aNo errors of rotational constants were derived because the band is perturbed (see the text).

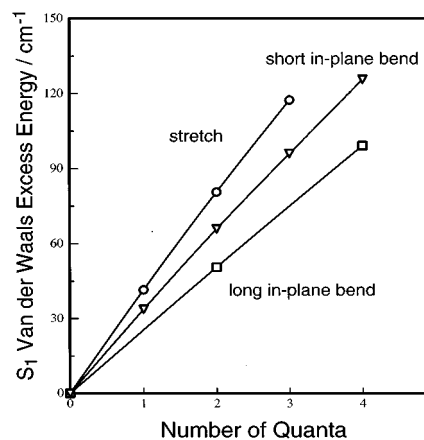


FIG. 8. S_1 vdW excess energy as a function of excited quanta of the vdW stretching modes, the short in-plane bending modes, and the long in-plane bending modes. The solid line represents a spline interpolation of the experimental points.

For molecules with a plane of symmetry and when the only out-of-plane atoms are symmetrically equivalent pairs, harmonic and/or anharmonic contributions to the pseudoinertial defect can be classified⁴¹ as due to (i) *symmetric* or *antisymmetric* vibrations (with respect to the plane of symmetry) of (ii) either *in-plane* or *out-of-plane* atoms. Since in *p*DFB–Ar there exist the *xz* and *yz* planes of symmetry, we can use this concept to characterize the b_x and b_y vdW bending modes. It is found that, e.g., a b_x normal mode can in principle produce harmonic contributions to Δ_x via the anti-symmetric (with respect to the *yz* plane) vibrations of both in-plane and out-of-plane atoms involved. Furthermore, it is seen that a b_x normal mode also affects Δ_y via harmonic and anharmonic contributions from the symmetric (with respect to the *xz* plane) vibrations of the out-of-plane atoms involved.

In order to extract information on mode character from experimental data in the electronically excited state, we consider instead of the pseudoinertial defect the quantity δP_x^{eff} , which we define as

$$\delta P_x^{\text{eff}} := P_x^{\text{eff}}(\text{vdW vibronic state}) - P_x^{\text{eff}}(0^0). \quad (3)$$

The numerical values of δP_x^{eff} and δP_y^{eff} evaluated for all vdW vibronic states are listed in Tables III–V. Large values ($|\delta P^{\text{eff}}| > 1$) indicate significant vibrational averaging. Small values of both δP_x^{eff} and δP_y^{eff} found for the s^1 and s^2 states (Table III). This means that these states represent nearly genuine stretching normal modes with negligible amplitudes in the (*x*,*y*) coordinates. For the b_x^2 state a large δP_y^{eff} ($= -19.926 \text{ u}\text{\AA}^2$) and a nearly zero δP_x^{eff} is found (Table V). Although a genuine b_x normal mode (with zero *y* amplitude) could, in principle, contribute to both δP_x^{eff} and δP_y^{eff} (as discussed for Δ_x and Δ_y), in our experiment a measurable effect is seen only for δP_y^{eff} . We take this as evidence for a genuine b_x motion in the sense that there is no amplitude in the other bending (b_y) direction (however, for b_x^2 there is an effect of bend–stretch coupling seen from δz_{eff} , see earlier text). The s^1 , s^2 , and b_x^2 states represent genuine normal modes and can thus be described by accurate vdW vibrational quantum numbers in a one-dimensional approximation (as mentioned earlier, for the b_x^2 state this is only true for the *x* and *y* coordinates). On the other hand, mode mixing is seen to be significant for higher energy vdW vibronic states, e.g., we find large values for δP_x^{eff} and δP_y^{eff} for the $s^1 b_x^2$ (Table V) or b_y^4 (Table IV) states. Therefore the assignments given in this work for these high energy vdW states have to be considered as linear approximation.

V. CONCLUSIONS

In this work, using sub-Doppler UV techniques with rotational resolution, the vdW vibronic spectrum of *p*DFB–Ar is measured up to an intermolecular excess energy of 125 cm^{-1} . This represents an expansion of directly excited vdW energy by a factor of 2 compared to previous results from vibrationally resolving techniques. For the assignment of the bands the identification and simulation of their rotational structure was inevitable. The transition frequencies obtained in this way show a regular behavior with moderate anharmonicities and no major perturbations of frequency positions due to anharmonic coupling. The latter mechanism couples the skeletal 30^1 state at $+119.880(15) \text{ cm}^{-1}$ and the s^3 vdW vibronic state at $+117.133(15) \text{ cm}^{-1}$, shifting the vdW state towards somewhat lower energies.

A major result of this work is the characterization of the mode character of excited vdW vibronic states. For this we interpreted the influence of vibration–rotation interaction by an analysis of effective planar moments. As a result we conclude that the vibrational motion in the s^1 and s^2 states leads to linear displacements along the *z* axis with negligible components along the *x* and *y* coordinates. Similarly, vibrational amplitude in the b_x^2 state contains no b_y character (although it contains some stretch displacement pointing to the librational character of the bending mode). Thus, for low energy states a simple one-dimensional harmonic picture seems to be adequate, in line with the small observed anharmonicities.

A different situation is found for higher energetic states, e.g., the b_y^4 state. Here considerable motional amplitude along the *x* and *y* coordinates is observed indicating that the vibrational state can no longer be considered as a pure b_y vibration in a one-dimensional picture.

In conclusion we have shown that rotationally resolved UV spectroscopy of van der Waals vibronic bands is useful for characterization of the intermolecular vibrational motion and the intermolecular potential. The measured rotational constants of the different vdW vibronic bands can provide a critical test of future results from 3D quantum mechanical bound state calculations based on theoretical model potentials.

ACKNOWLEDGMENTS

The authors are grateful to Professor E. W. Schlag for his continuous interest in this work. They thank R. Neuhauser for assistance and helpful discussions during the course of the experiments. Financial support from the Deutsche Forschungsgemeinschaft and the Fonds der Chemischen Industrie is gratefully acknowledged.

¹C. A. Haynam, D. V. Brumbaugh, and D. H. Levy, *J. Chem. Phys.* **80**, 2256 (1984).

²J. C. Alfano, S. J. Martinez III, and D. H. Levy, *J. Chem. Phys.* **94**, 1673 (1991).

³Th. Weber, A. von Bargaen, E. Riedle, and H. J. Neusser, *J. Chem. Phys.* **92**, 90 (1990).

⁴Th. Weber and H. J. Neusser, *J. Chem. Phys.* **94**, 7689 (1991).

⁵H. J. Neusser, R. Sussmann, A. M. Smith, E. Riedle, and Th. Weber, *Ber. Bunsenges. Phys. Chem.* **96**, 1252 (1992).

⁶S. M. Ohline, L. L. Connel, P. W. Joireman, V. A. Venturo, and P. M. Felker, *Chem. Phys. Lett.* **193**, 335 (1992).

⁷R. Sussmann and H. J. Neusser, *Chem. Phys. Lett.* **221**, 46 (1994).

⁸Structure of weakly bound complexes from electronic spectra: H. J. Neusser and R. Sussmann, in *Jet Spectroscopy and Molecular Dynamics*, edited by J. M. Hollas and D. Phillips (Chapman and Hall, London, 1994).

⁹R. Sussmann, U. Zitt, and H. J. Neusser, *J. Chem. Phys.* **101**, 9257 (1994).

¹⁰J. A. Menapace and E. R. Bernstein, *J. Phys. Chem.* **91**, 2533 (1987).

¹¹E. J. Bieske, M. W. Rainbird, I. M. Atkinson, and A. E. W. Knight, *J. Chem. Phys.* **91**, 752 (1989).

¹²M. Mons, J. Le Calvé, F. Piuzzi, and I. Dimicoli, *J. Chem. Phys.* **92**, 2155 (1990).

¹³J. J. F. Ramaekers, H. K. van Dijk, J. Langelaar, and R. P. H. Rettschnick, *Faraday Discuss. Chem. Soc.* **75**, 183 (1983).

¹⁴P. M. Weber, J. T. Buontempo, F. Novak, and S. A. Rice, *J. Chem. Phys.* **88**, 6082 (1988).

- ¹⁵ S. Leutwyler and J. Bösigler, *Chem. Rev.* **90**, 489 (1990).
- ¹⁶ S. Leutwyler, U. Even, and J. Jortner, *J. Chem. Phys.* **79**, 5769 (1983).
- ¹⁷ T. Troxler and S. Leutwyler, *J. Chem. Phys.* **95**, 4010 (1991).
- ¹⁸ G. Brocks and T. Huygen, *J. Chem. Phys.* **85**, 3411 (1986).
- ¹⁹ J. W. I. van Bladel, A. van der Avoird, and P. E. S. Wormer, *J. Phys. Chem.* **95**, 5414 (1991).
- ²⁰ C. A. Schmuttenmaer, R. C. Cohen, and R. J. Saykally, *J. Chem. Phys.* **101**, 146 (1994).
- ²¹ G. Brocks and D. van Koeven, *Mol. Phys.* **63**, 999 (1988).
- ²² A. van der Avoird, *J. Chem. Phys.* **98**, 5327 (1993).
- ²³ J. Faeder, *J. Chem. Phys.* **99**, 7664 (1993).
- ²⁴ P. Parneix, N. Halberstadt, Ph. Brechignac, F. G. Amar, A. van der Avoird, and J. W. van Bladel, *J. Chem. Phys.* **98**, 2709 (1993).
- ²⁵ D. Consalvo, A. van der Avoird, S. Picirillo, M. Coreno, A. Giardini-Guidoni, A. Mele, and M. Snels, *J. Chem. Phys.* **99**, 8398 (1993).
- ²⁶ M. Mandziuk and Z. Bacic, *J. Chem. Phys.* **98**, 7165 (1993).
- ²⁷ M. Mandziuk, Z. Bacic, T. Droz, and S. Leutwyler, *J. Chem. Phys.* **100**, 52 (1994).
- ²⁸ D. V. Brumbaugh, J. E. Kenny, and D. H. Levy, *J. Chem. Phys.* **78**, 3415 (1983).
- ²⁹ A. R. Tiller and D. C. Clary, *J. Chem. Phys.* **92**, 5875 (1990).
- ³⁰ B. B. Champagne, D. F. Plusquellic, J. F. Pfanstiel, D. W. Pratt, W. M. van Herpen, and W. L. Meerts, *Chem. Phys.* **156**, 251 (1991).
- ³¹ E. Riedle, R. Sussmann, Th. Weber, and H. J. Neusser, *J. Chem. Phys.* (submitted).
- ³² R. Sussmann, R. Neuhauser, and H. J. Neusser, *Can. J. Phys.* **72**, (1994).
- ³³ R. Sussmann, R. Neuhauser, and H. J. Neusser, *Chem. Phys. Lett.* **229**, 13 (1994).
- ³⁴ P. Hobza, H. L. Selzle, and E. W. Schlag, *J. Chem. Phys.* **95**, 391 (1991).
- ³⁵ B. A. Jacobson, S. Humphrey, and S. A. Rice, *J. Chem. Phys.* **89**, 5624 (1988).
- ³⁶ M.-C. Su, H.-K. O, and C. S. Parmenter, *Chem. Phys.* **156**, 261 (1991).
- ³⁷ A. E. W. Knight and S. H. Kable, *J. Chem. Phys.* **89**, 7139 (1988).
- ³⁸ W. Gordy and R. L. Cook, *Microwave Molecular Spectra*, 3rd ed. (Wiley-Interscience, New York, 1984), Chap. XIII.
- ³⁹ M. Mons and J. Le Calvé, *Chem. Phys.* **146**, 195 (1990).
- ⁴⁰ H. A. Jahn, *Phys. Rev.* **56**, 680 (1939).
- ⁴¹ D. R. Herschbach and V. W. Laurie, *J. Chem. Phys.* **40**, 3142 (1964).
- ⁴² T. Cvitas and J. M. Hollas, *Mol. Phys.* **18**, 793 (1970).